Research Article

Yan Kong#, Xiaoxuan Tang#, Yahong Zhao, Xiaoli Chen, Ke Yao, Liling Zhang, Qi Han, Luzhong Zhang, Jue Ling*, Yongjun Wang*, and Yumin Yang*

Degradable tough chitosan dressing for skin wound recovery

https://doi.org/10.1515/ntrev-2020-0105
received November 18, 2020; accepted December 9, 2020

Abstract: The performance of wound dressing determines the effect of wound closure and recovery. Water absorption and bacteriostasis of wound dressings play an important role in wound recovery and healing. In this study, an optimized chitosan wound dressing-tough chitosan dressing (TCS) with high water absorption, high bacteriostasis, and degradability was developed. The chemical structure of chitosan remained stable during the process of optimized treatment, and an increase in mechanical properties was obtained for the dressing. After optimization, the water absorption and antibacterial properties of the chitosan dressing were greatly improved, which is significantly better than sodium alginate dressing. The authors believe that TCS dressing with high hygroscopicity and high bacteriostasis has great potential application value in the field of wound recovery and healing.

Keywords: skin wound dressing, chitosan, hygroscopicity, bacteriostasis

1 Introduction

Skin trauma is one of the most common injuries in humans [1], which is painful and would cause wound infections by breaking the integrity and protective function of the skin. The recovery of skin traumatic wounds affects the patient's physical and mental condition. The implications of effective wound healing for both the patient and the economy are massive [2], and how to accelerate the healing of wounds was a focus question. Thus, the design of new wound materials is an urgent need for the development of modern medical technology [3,4].

In general, traditional dressings cannot provide a moist environment and play a bacteriostatic role in the wound [5]. Gauze, as a traditional wound dressing, could provide some protection for skin traumatic wounds, but their hydrophilicity was poor [6]. Hydrogel dressings possess excellent hydrophilicity and can provide a soothing and cooling effect to decrease the temperature of cutaneous wounds [7]. However, the exudate will lead to maceration and bacterial proliferation of the hydrogel dressings [8]. Alginate dressing has good biodegradability and hydrophilicity, which can stimulate macrophages to initiate an inflammatory response and accelerate wound healing [9]. However, the bacteriostatic effect of alginate dressing was poor [10]. Collagen dressings could greatly simulate the extracellular matrix, creating a physiological interface between the wound surface and the environment to promote wound healing [11,12]. However, allogeneic or heterogeneous collagen may cause immune rejection [13]. Nanosilver dressing is excellent in antibacterial wounds but may accumulate in the body by crossing the skin and mucous membrane barrier and cause damage to the human body [14]. The performance of wound dressing could be greatly improved by not only maintaining moisture at the wound site but also providing antibacterial

# These authors contributed equally to this work.

* **Corresponding author: Jue Ling,** Key Laboratory of Neuroregeneration of Jiangsu and Ministry of Education, Nantong University, 226001, Nantong, China, e-mail: jl2016@ntu.edu.cn
* **Corresponding author: Yongjun Wang,** Key Laboratory of Neuroregeneration of Jiangsu and Ministry of Education, Nantong University, 226001, Nantong, China, e-mail: wyjbs@ntu.edu.cn
* **Corresponding author: Yumin Yang,** Key Laboratory of Eco-Textiles, Ministry of Education, College of Textile Science and Engineering, Jiangnan University, Wuxi, Jiangsu 214122, China; Key Laboratory of Neuroregeneration of Jiangsu and Ministry of Education, Nantong University, 226001, Nantong, China, e-mail: yangym@ntu.edu.cn
Yan Kong: Key Laboratory of Eco-Textiles, Ministry of Education, College of Textile Science and Engineering, Jiangnan University, Wuxi, Jiangsu 214122, China
Xiaoxuan Tang, Yahong Zhao, Xiaoli Chen, Ke Yao, Liling Zhang, Qi Han, Luzhong Zhang: Key Laboratory of Neuroregeneration of Jiangsu and Ministry of Education, Nantong University, 226001, Nantong, China

effects to protect the wound from infection to promote wound healing [15].

To meet the needs of developing ideal wound dressings, nanotechnology-based materials have been attractive to researchers in the field of biomedical materials [16,17]. Because of the similarity in morphology and structure between the nanofibers and the natural extracellular matrix proteins, the nanofibers have certain promoting effects on the recovery of damaged tissues [18]. Particularly for wound healing, the nanofiber dressing prepared by electrospinning technology has excellent performance on promoting skin regeneration in wound treatment [19,20], because it could promote cell proliferation and migration [21]. The reinforced fiber with nanoparticles can effectively improve the mechanical properties and biological effects of the fiber surface, which is more conducive to cell growth [22].

As a natural polysaccharide substance, chitosan has various physiological functions such as biocompatibility, non-toxicity, and bacteriostasis [23,24]. Therefore, chitosan has been widely used in tissue engineering materials, medical fibers, antibacterial agents, drug sustained-release materials, and many other fields and other daily chemical industries [25,26]. The capacity of chitosan on promoting wound healing and hemostasis has been reported [27]. As a tissue engineering material, chitosan can also promote cell proliferation and tissue regeneration [28,29]. Its degradation product, chitosan oligosaccharides, also has excellent biological functions on tissue regeneration [30,31]. Among the dressing materials manufactured in recent years, chitosan dressing with biocompatibility has been considered as a dressing with promising applications [32,33]. However, chitosan materials have poor degradation performance under general conditions, which hinders their application [34].

To solve the disadvantages that traditional skin dressings cannot provide a moist environment, weak water absorption, and weak bacteriostasis ability, an optimized chitosan wound dressing was prepared in this study. The chitosan dressing was treated by the protonation reaction to obtain the TCS dressing with high water absorption, high bacteriostasis, and degradability. This optimized chitosan dressing could be considered as an excellent dressing candidate in practical applications.

2 Materials and methods

2.1 Preparation of chitosan dressing

The experiment used a protonation reaction in a non-aqueous system to make the chitosan carry positive ions. First, 100 g of chitosan (average MW = 9,000, commercial available) was immersed in 100 mL of ethanol, and 80 g of 75% acetic acid was slowly added dropwise, then reacted at room temperature for 3–4 h after stirring. After filtering and drying, optimized chitosan could be obtained. Dressings were fabricated using nonwoven technology [35]. Ordinary chitosan nonwoven dressing was used as a control. For ease of reference, the untreated chitosan dressing and treated chitosan dressing were named as UTCS and TCS dressings, respectively.

2.2 Scanning electron microscopy analysis

The surface of chitosan dressing was observed by electron microscope before and after optimization. Appropriate amount of flat dressing was cut, dried, and then sprayed with gold for observation under an electron microscope. By observing the morphology of the fiber and counting the diameter of the fiber, the effect of optimization treatment on the chitosan fiber was analyzed.

2.3 Fourier transform infrared analysis

Take the appropriate amount of UTCS and TCS for Fourier transform infrared (FTIR) spectroscopy to analyze the component. First, the dried dressing was cut and grind, and some potassium bromide was added. The mixture was then extruded into flakes and placed in a FTIR spectrometer for analysis. The experiment compared the obtained infrared spectrum curves and analyzed whether the optimization treatment would affect the composition of the chitosan dressing.

2.4 Mechanical analysis

In the experiment, the tensile mechanical analysis of the UTCS and TCS dressings was performed, and the

commercialized alginate dressing was selected as a comparison to evaluate the mechanical properties of the samples. The mechanical testing device was used to analyze the tensile strength of the dressing, and five parallel samples were set in each group to reduce the experimental error.

2.5 Wettability

The contact angle instrument was used to measure the hydrophilicity of different chitosan dressing. The contact angle of the chitosan dressing was measured under wet conditions. The dressing samples were placed on the contact angle test bench to measure the wettability, and the situation of water droplets on the material was observed from a top view. In this experiment, five parallel samples were used for each group.

2.6 Swelling test

The swelling rate of UTCS, TCS, and commercial control dressings was measured in the swelling test experiment.

The three kinds of dressings were cut to the 1×1 cm size, and three parallel samples were set in each group. The weight (m_1) of each sample was recorded separately, then the sample was immersed in phosphate buffer saline (PBS), and the swelling experiment was performed at room temperature. The time points of 10, 20, 30 min, 1, 1.5, 2, 3, 4, 6, 12, 24, 48, 72, and 96 h were set in the experiment. At each time point, the excess PBS was discarded and the weight (m_t) of each sample was recorded. The calculation method of swelling rate was:

$$\frac{m_t - m_1}{m_1} \times 100\%.$$

2.7 Degradation

The PBS solution was used to analyze the degradation of the dressing *in vitro*. The weight of each sample was recorded at the beginning of the experiment (m_1), and then the samples were soaked in 3 mL of PBS and incubated at 37°C. The samples were taken out at the time point (1, 3, 5, 7, 10, and 15 days), the lyophilized weight of samples (m_t) was recorded, and three parallel samples were set at each time point. The degradation rate was calculated by the following equation:

$$\frac{m_1 - m_t}{m_1} \times 100\%.$$

2.8 Antibacterial test

The modified chitosan powder (I) and commercial bacteriostatic powder (II) were formulated into the concentration of 32,000 μg/mL with 0.5% acetic acid solution as the original solution. The concentrations of 16,000, 8,000, 4,000, 2,000, 1,000, 500, 250, 125, 62.5, and 31.25 μg/mL were diluted in 96-well plates. The volume of solution in each well was 100 μL. Then another 100 μL of bacterial solution (OD 600 = 0.5) was added to each well. Only culture medium was added as a control group. Three strains of *Staphylococcus aureus*, *Escherichia coli*, and *Candida albicans* were inoculated separately, and each drug concentration was repeated thrice. After shaking culture for 18 h, the microplate reader read the absorbance at 600 nm.

Then, the antibacterial properties between chitosan powder and chitosan nonwoven dressing were tested. The bacteriostatic difference between the two groups was analyzed by counting the number of colonies formed after cultivation. The bacterial liquid without adding sample was treated in the same way and used as a negative control.

After that, the commercial sodium alginate (SA) wound dressing was then used as a control to evaluate the antibacterial properties of the chitosan dressing. The UTCS dressing (1), TCS dressing (2), and SA commercial wound dressing (3) were cut to the same size (1×0.5 cm). Then, the samples were immersed in the bacterial culture medium. The bacterial liquid without adding dressing was treated in the same way and used as a negative control. Three strains of *S. aureus*, *E. coli*, and *C. albicans* were used for the experiment, and each experiment was repeated thrice. The number of colony-forming unit was counted after overnight cultivation. Finally, the following equation was used to calculate the antibacterial rate %:

$$\text{Antibacterial rate \%} = \frac{\text{number of colonies in the control group} - \text{number of colonies in the experimental group}}{\text{number of colonies in the control group}} \times 100\%.$$

2.9 Statistical analysis

All data analyses were performed with GraphPad Prism. Differences between the experimental groups were analyzed and compared by *t*-test analysis of variance. Statistical significance was designated with $*P < 0.05$, $**P < 0.01$, and $***P < 0.001$.

3 Results and discussion

3.1 Morphology of the dressing

In this study, chitosan powder was dispersed in ethanol by dropwise addition of acetic acid. In this process, the amino groups of chitosan were protonated and possessed positive charges in acidic solutions with improved hydrophilicity [36]. Then, positive charged chitosan powder was obtained after filtration. Then, TCS dressing was prepared by nonwoven technology.

To investigate the microstructure of the dressings, scanning electron microscopy (SEM) analysis was conducted [37]. The morphologies and diameter distributions of chitosan dressing before and after treatment are shown in Figure 1. As shown in SEM images, the fibers of both UTCS and TCS dressings were smooth, cylindrical, and randomly oriented (Figure 1a). There was no significant difference between UTCS and TCS on the macroscopic morphology (Figure 1b). The fiber diameter of UTCS dressing was 12.09 ± 0.5937 μm (Figure 1c). The average fiber diameter of TCS dressing was 13.36 ± 0.4523 μm (Figure 1c), which is very close to that of UTCS dressing with no statistical difference.

3.2 FTIR analysis

To determine the composition of chitosan dressings, we characterized their chemical structures by FTIR analysis. The characteristic peaks of chitosan were all found in the FTIR spectra of both UTCS and TCS in Figure 2. The peak in absorbance at 3,450 and 2,867 cm^{-1} represents O–H group and C–H stretch, respectively. The peak at 1,071 cm^{-1} represents skeletal vibration involving bridge C–O stretch and 1,375 cm^{-1} represents asymmetric C–H

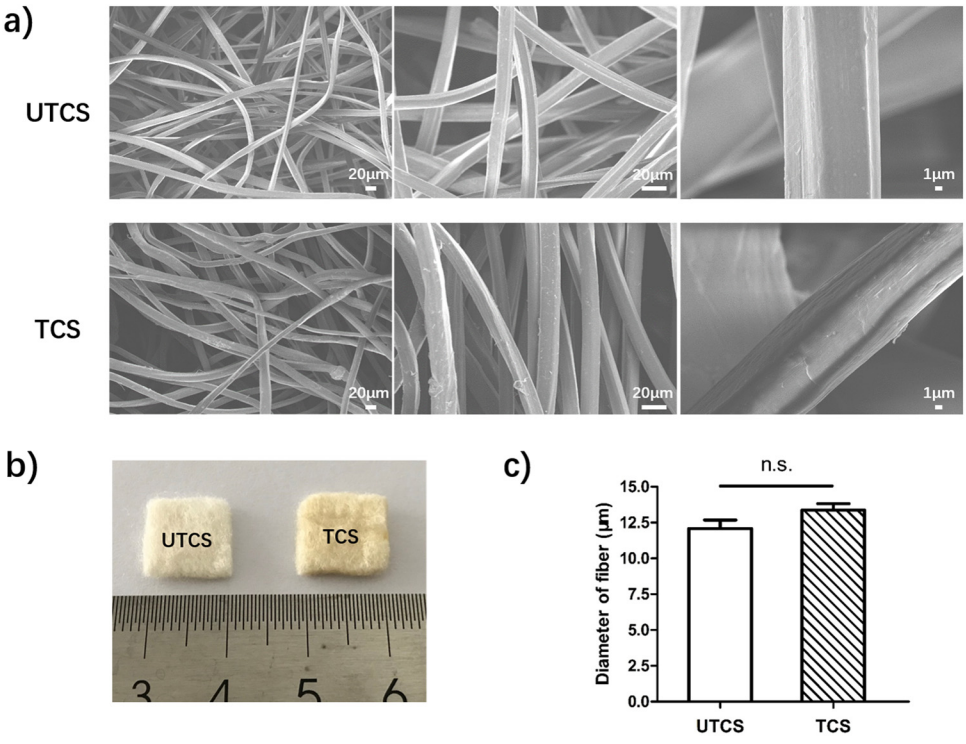

Figure 1: (a) Scanning electron micrograph of UTCS and TCS dressings; (b) macro photographs of UTCS and TCS dressings; (c) statistical analysis of the fiber diameter of two groups ($n = 30$). All data were mean ± SEM. The differences in each group were performed using two-tailed unpaired *t*-test. NS indicates $P > 0.05$.

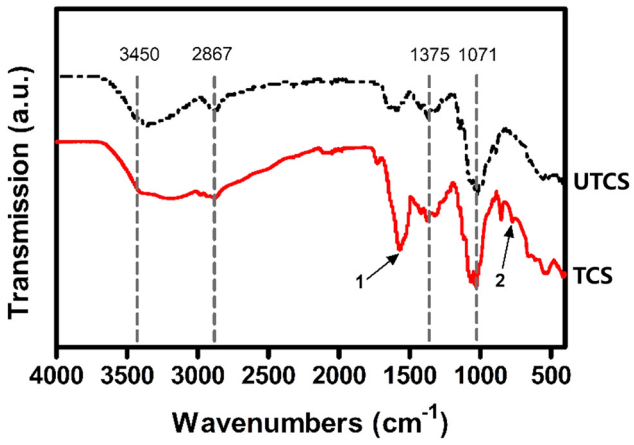

Figure 2: FTIR spectra of the chitosan dressing before and after optimization.

bending of CH_2 group [38]. This indicates that the optimization process did not change the original main ingredients of the chitosan dressing. It is also worth noting that the peaks indicated by arrows 1 and 2 appear only in the infrared curve of the TCS group, which may be caused by the protonation of amino groups and free H ions or residual acetic acid, respectively.

3.3 Mechanical tensile test

Excellent mechanical properties are required for developing desirable wound dressing to maintain integrity and protect the damaged area under external forces [39]. Therefore, tensile tests were performed to determine the stretchability of wound dressings of varied compositions. The results showed that the SA wound dressing ruptured easily at small loads strains of 2.351 N. The UTCS ruptured at 8.098 N. The Young's modulus of UTCS was basically the same as the SA dressing (0.396 MPa), which was 0.369 MPa (Figure 3d). In contrast, TCS sustained loads of 21.5 N without rupture and had the highest mechanical strength (1.078 MPa) in comparison to UTCS (0.405 MPa) and SA (0.118 MPa) groups. Moreover, the young's modulus of TCS (3.29 MPa) was significantly higher than UTCS (0.369 MPa) and SA (0.396 MPa). After the optimization, the mechanical properties of the chitosan dressing were significantly enhanced. Study had shown that the shear force is the main reason to destroy the structure of nanofibers [40]. It may be that after optimizing the treatment process, the chitosan fiber becomes very easy to absorb water. After the dressing was dried again, the dressing was tougher because the chitosan

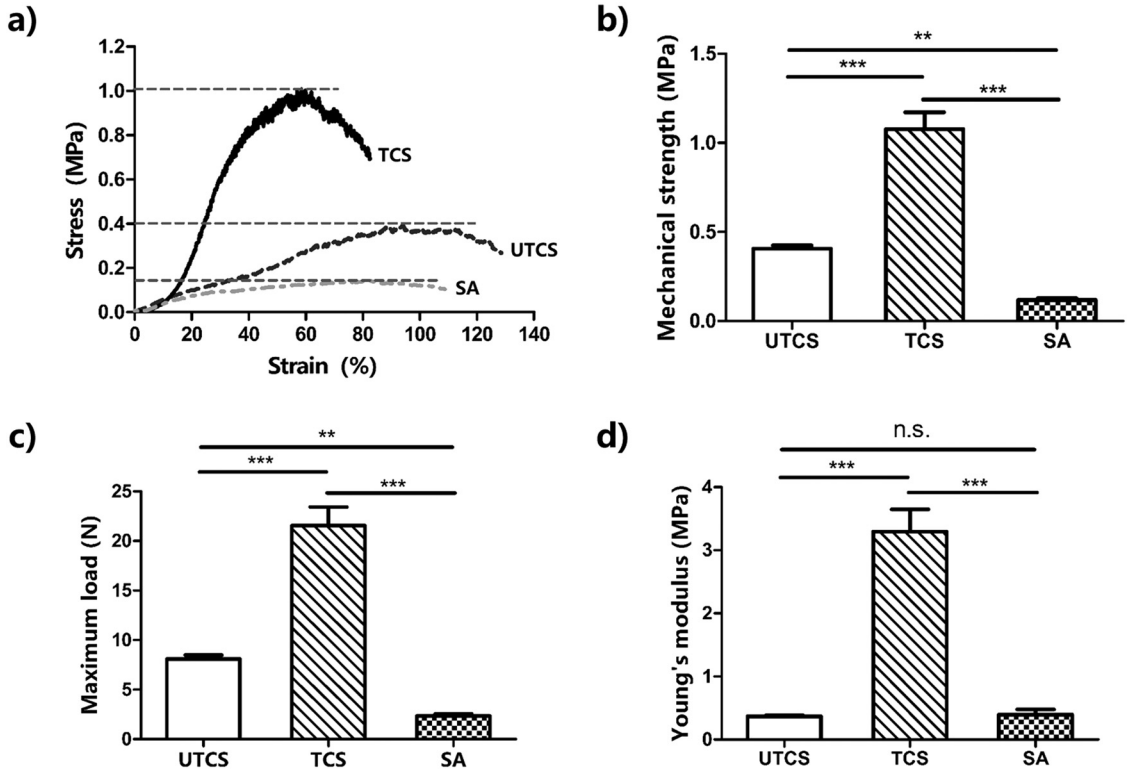

Figure 3: Mechanical test of the wound dressing: (a) the stress–strain curve of the dressing; (b) mechanical strength of dressing ($n = 5$); (c) maximum load of the dressing ($n = 5$); (d) Young's modulus for each dressing ($n = 5$). All data were mean ± SEM. The differences in each group were performed using two-tailed unpaired *t*-test. NS indicates $P > 0.05$. $^{**}P < 0.01$ and $^{***}P < 0.001$.

fibers became tighter and could bear greater shearing force. In general, the Young's modulus of human skin is about 0.5–2 MPa [41]. Therefore, the Young's modulus (3.29 MPa) of TCS dressing could meet the needs of the requirement of large motion when applied to wound sites.

3.4 Wettability analysis

Because the surface wettability significantly influences the biocompatibility of dressings exposed to tissue, we determined the contact angle of the chitosan dressings and compared with that of SA dressing. Figure 4 shows the droplet from the side view in contact angle analysis. The water droplets rapidly infiltrated and spread out on the surface of UTCS, TCS, and SA dressings without showing the contact angle after dropped on the dressing. Both UTCS and TCS groups showed comparable hydrophilicity to SA dressing under wetting conditions, which is because of the fact that chitosan itself is a hydrophilic substance. These results suggest that TCS could absorb exudative tissue fluid at the wound site effectively.

3.5 Swelling capacity and degradation

The capability of retaining and absorbing water is a significant parameter to evaluate its application in wound dressing field. It would prohibit the accumulation of exudates at the wound site and could absorb nutrition into the dressing [42]. Therefore, the ideal wound dressing should have excellent water retention ability and swelling rate to maintain a moist healing environment to promote wound healing [43].

Figure 5 shows the swelling ratio of wound dressing from different groups. The swelling rate of all groups increased significantly within 10 min. However, the UTCS group reached its maximum swelling rate after 10 min. In contrast, both the TCS and SA groups reached their maximum swelling after 48 h. The highest swelling ratio of 2,100% was observed in the TCS group, whereas UTCS dressing showed the least swelling ratio of 300%. The final swelling rate of SA dressing was between the other two groups (850%). Besides, after soaked in PBS for 2 h, the volume of TCS dressing was enlarged. The appearance of it became transparent and moist. The water was fully absorbed and wrapped by the TCS group. TCS dressing has a better ability to absorb the water which could reach twice the SA dressing because of the protonation of the chitosan in optimized dressing. This property was effective in cleaning a wound with a large amount of exudate.

The degradation analysis of three wound dressings was performed by PBS (Figure 5). Soaking in PBS for 15 days, the dry weight degradation rate of UTCS, TCS, and SA was 1.64, 43.01, and 49.97%, respectively. Clearly, the UTCS group showed no degradation basically (<5%) at the end of the analysis, and the degradation rate of the TCS (>40%) was significantly higher than that of UTCS. These results were in line with the results of the swelling rate shown in Figure 5b. The increased degradation rate of TCS was because the chitosan becomes more soluble in water after protonation on the amino group of the chitosan. The TCS has the same degradation tendency (43.01%) as the commercial SA dressing (49.97%), and there is no significant difference in the final degradation rate between them. Therefore, the chitosan dressing (TCS) prepared in this experiment achieved excellent degradation performance, which could match the degree of wound healing better. This degradation characteristic makes the TCS dressing have the potential for clinical application.

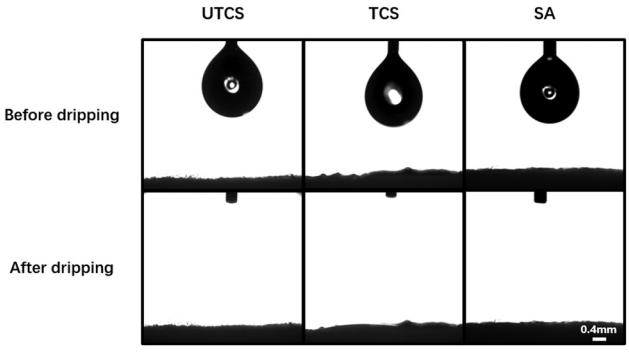

Figure 4: The contact angle of three dressings under wetting conditions before and after water drop. Scale bars represent 0.4 mm.

3.6 Antibacterial experiment

Because of the lack of skin protection at the wound, the defected sites are easy to be infected by various bacteria from the outside; therefore, the antibacterial effect of the dressing on bacteria is very important for the recovery of the wound [44]. Optimum wound healing dressing that has inherent antibacterial properties will be more

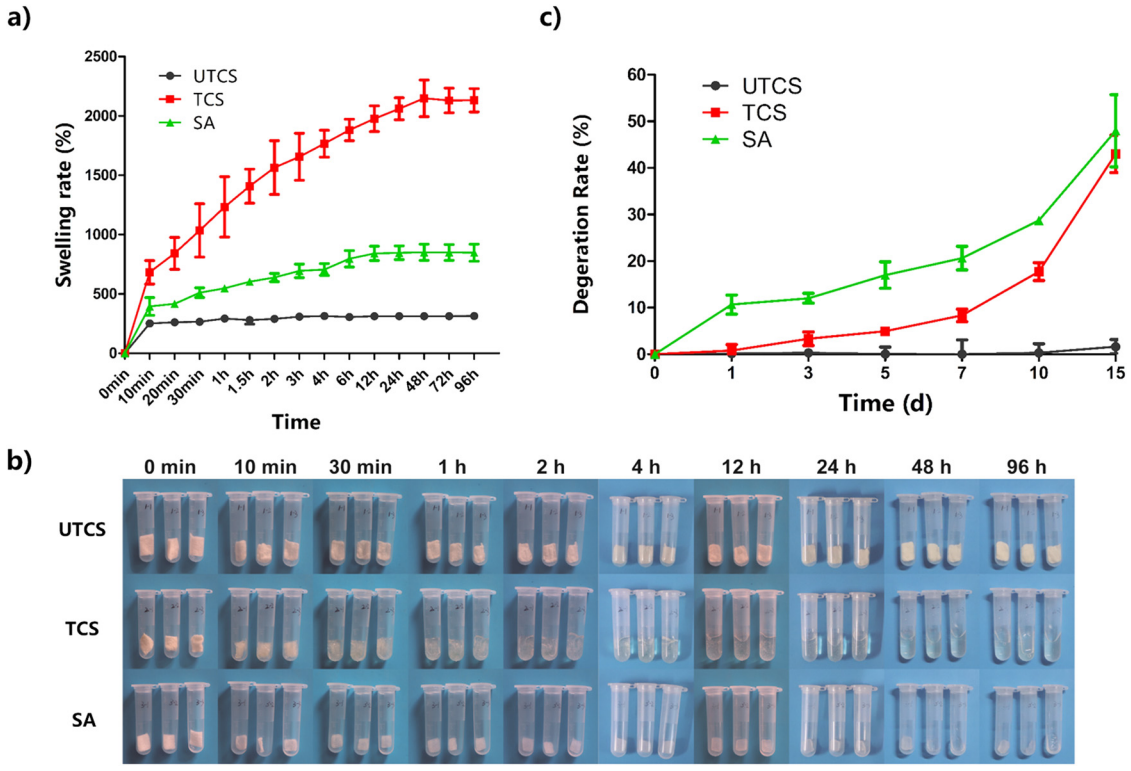

Figure 5: (a) Swelling curves of three different dressings; (b) swelling behavior of three dressings in PBS; (c) degradation of three dressings within 15 days. Each group had three parallel samples (n = 3). All data were mean ± SEM.

attractive to play the role of barrier to protect the wound tissue from external bacterial infection [45].

In this study, the antibacterial activities of all wound dressing were evaluated using *E. coli*, *S. aureus*, and *C. albicans*. In Figure 6a and b, the powder of TCS (I) exhibited an excellent antibacterial rate (>95%) for *S. aureus*, *E. coli*, and *C. albicans*, indicating its outstanding inherent antibacterial properties. The antibacterial rates of commercial bacteriostatic powder (II) for the three strains hovered around 80%. Obviously, the antibacterial effect of TCS dressing powder was better than that of commercial antibacterial powder. This is because chitosan itself has excellent antibacterial properties, and its positively charged amino group may damage the bacterial cell wall, resulting in the release of bacterial intracellular fluid, thereby playing a bactericidal role [1,46].

Figure 6c compares the antibacterial efficiency of TCS dressing in different forms. Regardless of the form of powder or complete excipients, their antibacterial rate for the three strains all reached 90% with no significant difference. Next, the UTCS, TCS, and SA dressings were compared for bacteriostatic effects (Figure 6d). From the perspective of the number of colonies of different bacterial species, the number of colonies on the optimized chitosan dressing group was greatly reduced, and the bacteriostatic rate was above 90%. Figure 6e shows that the antibacterial rate of the UTCS group was lower than that of the TCS group. This showed that the optimized treatment process could effectively improve the antibacterial ability of chitosan dressing. In contrast, in the SA group, the bacteriostatic rates of the three strains were all below 20%. This is because SA does not have inherent antimicrobial properties [47].

Chitosan itself has better antibacterial properties than SA materials, but the chitosan does not diffuse well in the bacterial solution before optimization. The optimized antibacterial effect of chitosan dressing can be attributed to the excellent water absorption and swelling of TCS dressing. Optimizing the chitosan dressing could absorb more culture fluid, which made it easier to spread in the bacterial solution, thus improving the bacteriostatic efficiency. Obviously, the TCS dressing was better than the other two groups. It is worth mentioning that the antibacterial effect of optimized chitosan against *C. albicans* was close to 100%, which had a significant advantage compared to the other two dressings. To sum up, this chitosan dressing with superior antibacterial properties has potential value as a clinical dressing.

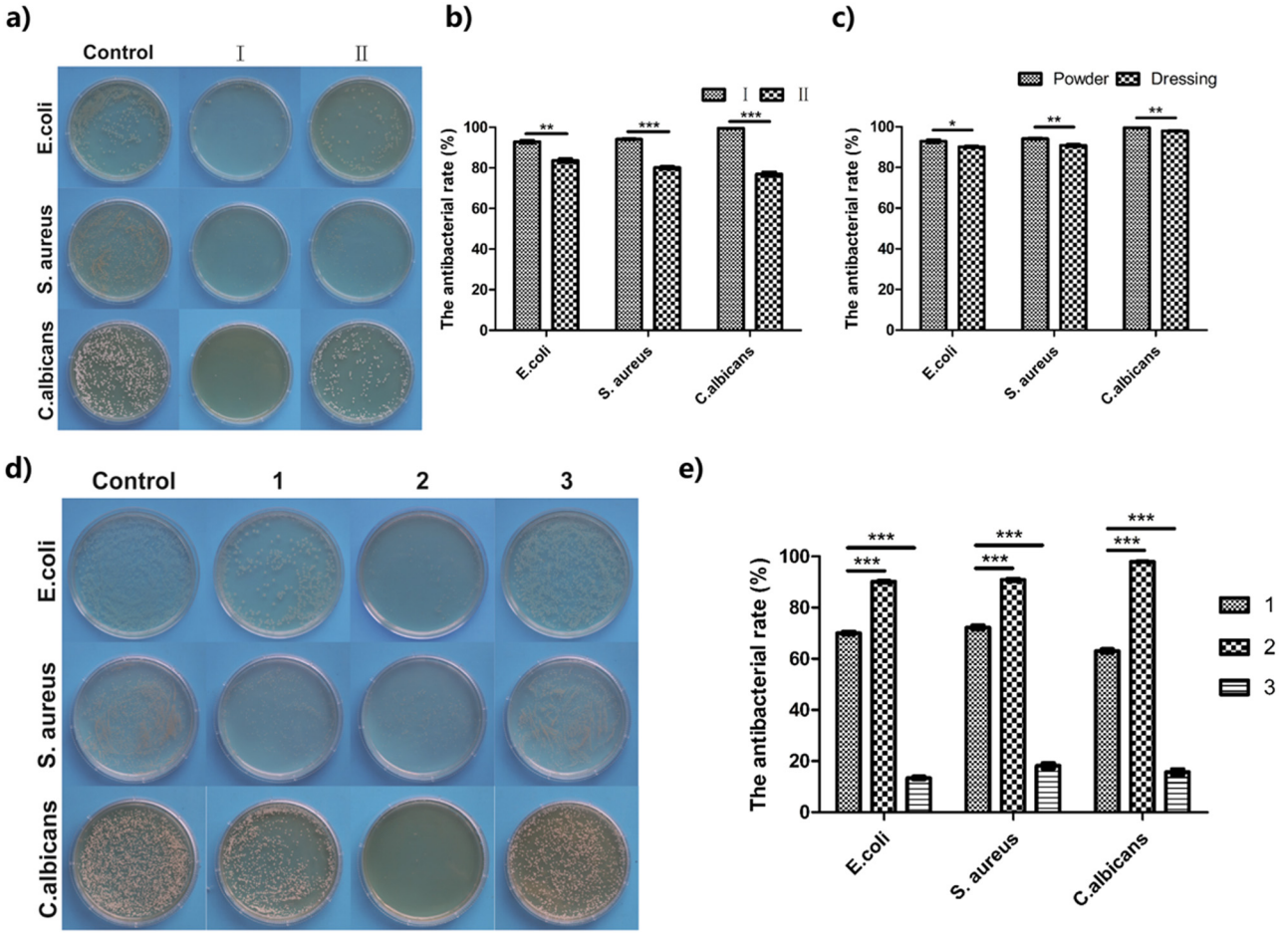

Figure 6: Antibacterial experiment of various dressings: (a and b) antibacterial experiment of chitosan in powder state, I: TCS powder, II: commercial antibacterial powder ($n = 5$); (c) antibacterial effect of TCS in different forms ($n = 5$); (d and e) antibacterial effect of various dressings on three bacterial species. 1: UTCS dressing; 2: TCS dressing; 3: SA wound dressing. $n = 5$ in each group. The differences between each group were performed using two-tailed unpaired *t*-test. $^*P < 0.05$, $^{**}P < 0.01$, and $^{***}P < 0.001$.

4 Conclusion

To solve the poor degradability of chitosan dressing and improve the water absorption and antibacterial properties of chitosan dressing, this experiment prepared a chitosan dressing with degradable, ultra-high water absorption, high antibacterial properties, and excellent mechanical properties to meet the urgent needs of developing desirable wound materials. So as to meet the urgent needs of developing desirable wound materials, the water absorption of TCS dressing can reach 2,100% and the improved mechanical properties of TCS dressing were achieved. In terms of bacteriostasis, the bacteriostatic effect of TCS dressing is significantly better than the commercial SA dressing. The TCS dressing has certain application potential and value in the treatment of wound injury and healing process.

Acknowledgments: Y. Kong and X. Tang contributed equally to this work. The authors gratefully acknowledge the financial support of the National Key Research and Development Program of China (2018YFC1105600).

Conflict of interest: The authors declare no conflict of interest regarding the publication of this paper.

References

[1] Qu J, Zhao X, Liang YP, Zhang TL, Ma PX, Guo BL. Antibacterial adhesive injectable hydrogels with rapid self-healing, extensibility and compressibility as wound dressing for joints skin wound healing. Biomaterials. 2018;183:185–99.

[2] Rosenbaum AJ, Banerjee S, Rezak KM, Uhl RL. Advances in wound management. J Am Acad Orthop Sur. 2018;26(23):833–43.

[3] Annabi N, Rana D, Shirzaei Sani E, Portillo-Lara R, Gifford JL, Fares MM, et al. Engineering a sprayable and elastic hydrogel adhesive with antimicrobial properties for wound healing. Biomaterials. 2017;139:229–43.
[4] Guo B, Ma PX. Conducting polymers for tissue engineering. Biomacromolecules. 2018;19(6):1764–82.
[5] Ghomi ER, Khalili S, Khorasani SN, Neisiany RE, Ramakrishna S. Wound dressings: Current advances and future directions. J Appl Polym Sci. 2019;136(27):47738.
[6] Dhivya S, Padma VV, Santhini E. Wound dressings – a review. Biomedicine (Taipei). 2015;5(4):22.
[7] Koehler J, Brandl FP, Goepferich AM. Hydrogel wound dressings for bioactive treatment of acute and chronic wounds. Eur Polym J. 2018;100:1–11.
[8] Tao G, Cai R, Wang YJ, Liu LY, Zuo H, Zhao P, et al. Bioinspired design of AgNPs embedded silk sericin-based sponges for efficiently combating bacteria and promoting wound healing. Mater Des. 2019;180:107940.
[9] Koga AY, Pereira AV, Lipinski LC, Oliveira MRP. Evaluation of wound healing effect of alginate films containing Aloe vera (Aloe barbadensis Miller) gel. J Biomater Appl. 2018;32(9):1212–21.
[10] Tang XX, Gu XY, Wang YL, Chen XL, Ling J, Yang YM. Stable antibacterial polysaccharide-based hydrogels as tissue adhesives for wound healing. Rsc Adv. 2020;10(29):17280–7.
[11] He Y, Hou Z, Wang J, Wang Z, Li X, Liu J, et al. Assessment of biological properties of recombinant collagen-hyaluronic acid composite scaffolds. Int J Biol Macromol. 2020;149:1275–84.
[12] Muthukumar T, Sreekumar G, Sastry TP, Chamundeeswari M. Collagen as a potential biomaterial in biomedical applications. Rev Adv Mater Sci. 2018;53(1):29–39.
[13] Palchesko RN, Carrasquilla SD, Feinberg AW. Natural biomaterials for corneal tissue engineering, repair, and regeneration. Adv Healthc Mater. 2018;7(16):1701434.
[14] Abdelsalam M, Al-Homidan I, Ebeid T, Abou-Emera O, Mostafa M, Abd El-Razik M, et al. Effect of silver nanoparticle administration on productive performance, blood parameters, antioxidative status, and silver residues in growing rabbits under hot climate. Animals-Basel. 2019;9(10):845.
[15] Tao G, Wang YJ, Cai R, Chang HP, Song K, Zuo H, et al. Design and performance of sericin/poly(vinyl alcohol) hydrogel as a drug delivery carrier for potential wound dressing application. Mat Sci Eng C Mater. 2019;101:341–51.
[16] Shi LX, Liu X, Wang WS, Jiang L, Wang ST. A Self-pumping dressing for draining excessive biofluid around wounds. Adv Mater. 2019;31(5):1804187.
[17] Alves P, Santos M, Mendes S, Miguel SP, de Sa KD, Cabral CSD, et al. Photocrosslinkable nanofibrous asymmetric membrane designed for wound dressing. Polymers-Basel. 2019;11(4):653.
[18] Sun XM, Bai Y, Zhai H, Liu S, Zhang C, Xu YW, et al. Devising micro/nano-architectures in multi-channel nerve conduits towards a pro-regenerative matrix for the repair of spinal cord injury. Acta Biomater. 2019;86:194–206.
[19] Levengood SL, Erickson AE, Chang FC, Zhang M. Chitosan-poly (caprolactone) nanofibers for skin repair. J Mater Chem B. 2017;5(9):1822–33.
[20] Amini F, Semnani D, Karbasi S, Banitaba SN. A novel bilayer drug-loaded wound dressing of PVDF and PHB/Chitosan nanofibers applicable for post-surgical ulcers. Int J Polym Mater Po. 2019;68(13):772–7.
[21] Zhang XL, Huang C, Zhao Y, Jin XY. Preparation and characterization of nanoparticle reinforced alginate fibers with high porosity for potential wound dressing application. Rsc Adv. 2017;7(62):39349–58.
[22] Deng Y, Yang WZ, Shi D, Wu MJ, Xiong XL, Chen ZG, et al. Bioinspired and osteopromotive polydopamine nanoparticle-incorporated fibrous membranes for robust bone regeneration. NPG Asia Mater. 2019;11:39.
[23] Muxika A, Etxabide A, Uranga J, Guerrero P, de la Caba K. Chitosan as a bioactive polymer: Processing, properties and applications. Int J Biol Macromol. 2017;105:1358–68.
[24] Guo SH, Fu DW, Utupova A, Sun DJ, Zhou M, Jin Z, et al. Applications of polymer-based nanoparticles in vaccine field. Nanotechnol Rev. 2019;8(1):143–55.
[25] Zhang L, Zhao WJ, Niu CM, Zhou YJ, Shi HY, Wang YL, et al. Genipin-cross-linked chitosan nerve conduits containing TNF-alpha inhibitors for peripheral nerve repair. Ann Biomed Eng. 2018;46(7):1013–25.
[26] Miao Y, Lu JW, Yin JH, Zhou CC, Guo YP, Zhou SM. Yb3+ -containing chitosan hydrogels induce B-16 melanoma cell anoikis via a Fak-dependent pathway. Nanotechnol Rev. 2019;8(1):645–60.
[27] Biranje SS, Madiwale PV, Patankar KC, Chhabra R, Dandekar-Jain P, Adivarekar RV. Hemostasis and anti-necrotic activity of wound-healing dressing containing chitosan nanoparticles. Int J Biol Macromol. 2019;121:936–46.
[28] Re F, Sartore L, Moulisova V, Cantini M, Almici C, Bianchetti A, et al. 3D gelatin-chitosan hybrid hydrogels combined with human platelet lysate highly support human mesenchymal stem cell proliferation and osteogenic differentiation. J Tissue Eng. 2019;10:2041731419845852.
[29] Lau YT, Kwok LF, Tam KW, Chan YS, Shum DKY, Shea GKH. Genipin-treated chitosan nanofibers as a novel scaffold for nerve guidance channel design. Colloid Surf B. 2018;162:126–34.
[30] Zhao YH, Wang YJ, Gong JH, Yang L, Niu CM, Ni XJ, et al. Chitosan degradation products facilitate peripheral nerve regeneration by improving macrophage-constructed microenvironments. Biomaterials. 2017;134:64–77.
[31] Wang YJ, Zhao YH, Sun C, Hu W, Zhao J, Li GC, et al. Chitosan degradation products promote nerve regeneration by stimulating schwann cell proliferation via miR-27a/FOXO1 axis. Mol Neurobiol. 2016;53(1):28–39.
[32] Hamedi H, Moradi S, Hudson SM, Tonelli AE. Chitosan based hydrogels and their applications for drug delivery in wound dressings: A review. Carbohyd Polym. 2018;199:445–60.
[33] Patrulea V, Ostafe V, Borchard G, Jordan O. Chitosan as a starting material for wound healing applications. Eur J Pharm Biopharm. 2015;97:417–26.
[34] Yan TT, Li CP, Ouyang QQ, Zhang DY, Zhong QK, Li PW, et al. Synthesis of gentamicin-grafted-chitosan with improved solubility and antibacterial activity. React Funct Polym. 2019;137:38–45.
[35] Kiyak Y, Maze B, Pourdeyhimi B. Microfiber nonwovens as potential membranes. Sep Purif Rev. 2019;48(4):282–97.
[36] Zhang Y, Liu BL, Wang LJ, Deng YH, Zhou SY, Feng JW. Preparation, structure and properties of acid aqueous solution

plasticized thermoplastic chitosan. Polymers-Basel. 2019;11(5):818.
[37] Hashim H, Salleh MS, Omar MZ. Homogenous dispersion and interfacial bonding of carbon nanotube reinforced with aluminum matrix composite: A review. Rev Adv Mater Sci. 2019;58(1):295–303.
[38] Ho TT, Bremmell KE, Krasowska M, MacWilliams SV, Richard CJ, Stringer DN, et al. In situ ATR FTIR spectroscopic study of the formation and hydration of a fucoidan/chitosan polyelectrolyte multilayer. Langmuir. 2015;31(41):11249–59.
[39] Annabi N, Rana D, Sani ES, Portillo-Lara R, Gifford JL, Fares MM, et al. Engineering a sprayable and elastic hydrogel adhesive with antimicrobial properties for wound healing. Biomaterials. 2017;139:229–43.
[40] Liu SD, Li DS, Yang Y, Jiang L. Fabrication, mechanical properties and failure mechanism of random and aligned nanofiber membrane with different parameters. Nanotechnol Rev. 2019;8(1):218–26.
[41] Fu RM, Tu LJ, Zhou YH, Fan L, Zhang FM, Wang ZG, et al. A tough and self-powered hydrogel for artificial skin. Chem Mater. 2019;31(23):9850–60.
[42] Sood N, Bhardwaj A, Mehta S, Mehta A. Stimuli-responsive hydrogels in drug delivery and tissue engineering. Drug Deliv. 2016;23(3):758–80.
[43] Qu J, Zhao X, Liang YP, Xu YM, Ma PX, Guo BL. Degradable conductive injectable hydrogels as novel antibacterial, anti-oxidant wound dressings for wound healing. Chem Eng J. 2019;362:548–60.
[44] Zhao X, Wu H, Guo BL, Dong RN, Qiu YS, Ma PX. Antibacterial anti-oxidant electroactive injectable hydrogel as self-healing wound dressing with hemostasis and adhesiveness for cutaneous wound healing. Biomaterials. 2017;122:34–47.
[45] Li X, Wu B, Chen H, Nan KH, Jin YY, Sun L, et al. Recent developments in smart antibacterial surfaces to inhibit biofilm formation and bacterial infections. J Mater Chem B. 2018;6(26):4274–92.
[46] Ali A, Ahmed S. A review on chitosan and its nanocomposites in drug delivery. Int J Biol Macromol. 2018;109:273–86.
[47] Chen K, Wang FY, Liu SY, Wu XF, Xu LM, Zhang DK. In situ reduction of silver nanoparticles by sodium alginate to obtain silver-loaded composite wound dressing with enhanced mechanical and antimicrobial property. Int J Biol Macromol. 2020;148:501–9.